

## Improvement of Voltammetric Detection of Sulfanilamide with a Nanodiamond-Modified Glassy Carbon Electrode

Hao Li<sup>1,\*</sup>, Ximmou Kuang<sup>1</sup>, Xiaolan Shen<sup>1</sup>, Jianwei Zhu<sup>1</sup>, Botao Zhang<sup>2,3,\*</sup>, Hua Li<sup>2,3,\*</sup>

<sup>1</sup> College of Chemical Engineering, Ningbo Polytechnic, No.388 East Lushan Road, Ningbo, 315800, China

<sup>2</sup> Key laboratory of Marine Materials and Related Technologies, Zhejiang Key Laboratory of Marine Materials and Protective Technologies, Ningbo Institute of Materials Technology and Engineering, Chinese Academy of Sciences, Ningbo 315201, China

<sup>3</sup> Cixi Institute of Biomedical Engineering, Ningbo Institute of Materials Technology and Engineering, Chinese Academy of Sciences, Ningbo 315201, China

\*E-mail: [2016121@nbpt.edu.cn](mailto:2016121@nbpt.edu.cn) (Hao Li); [zhangbotao@nimte.ac.cn](mailto:zhangbotao@nimte.ac.cn) (Botao Zhang); [lihua@nimte.ac.cn](mailto:lihua@nimte.ac.cn) (Hua Li)

Received: 10 April 2019 / Accepted: 25 May 2019 / Published: 30 June 2019

Owing to its high hardness, high chemical inertness, and good biocompatibility, nanodiamond (ND) has recently been increasingly used in electrochemical analysis. In this work, a comparative study of voltammetric detection of sulfanilamide using a bare glassy carbon electrode (GCE) and ND-modified glassy carbon electrode (GCE-ND) was carried out. Scanning electron microscopy (SEM) and cyclic voltammetry (CV) analyses revealed that modification of a GCE with 100  $\mu\text{L}$  of ND suspension (40  $\text{mg}\cdot\text{L}^{-1}$ ) was the optimum condition in this study. The results of CV analyses with the  $[\text{Fe}(\text{CN})_6]^{3-}$  redox couple suggested the occurrence of a diffusion-controlled process on both electrodes. However, the GCE-ND exhibited a larger electroactive surface area and a higher heterogeneous electron transfer rate constant, which were approximately 2.11 and 5.05 times greater than those of the bare GCE, respectively. When applied to the detection of sulfanilamide solution using square wave voltammetry under the optimum conditions, the bare GCE showed a linear dynamic range of 1–80  $\text{mg}\cdot\text{L}^{-1}$  ( $R^2 = 0.9994$ ) with a detection limit of 0.744  $\text{mg}\cdot\text{L}^{-1}$ , by contrast, the GCE-ND showed a linear dynamic range of 0.2–100  $\text{mg}\cdot\text{L}^{-1}$  ( $R^2 = 0.9949$ ) with a detection limit of 0.161  $\text{mg}\cdot\text{L}^{-1}$ . The detection limit of the GCE-ND was as much as 78.4% lower than that of the bare GCE. Furthermore, interday detection experiments revealed that the GCE-ND had higher repeatability and accuracy than the bare GCE.

**Keywords:** nanodiamond, glassy carbon electrode, sulfanilamide, square wave voltammetry

### 1. INTRODUCTION

Owing to their unique structure, excellent performance, and high chemical stability, nanocarbon materials have been ideal choices for electrochemical applications [1,2]; in particular, carbon nanotubes

[3] and graphene [4], which exhibit excellent conductivity, high specific surface areas, and three-dimensional network structures, have been extensively investigated in such applications. As a member of nanocarbon materials, nanodiamond (ND) also exhibits characteristics of the small size effect, surface effects, the quantum size effect, and the macro quantum tunnel effect [5]. In addition, ND displays high hardness, high chemical inertness, good biocompatibility, and low toxicity. Its surface contains several oxygen-containing groups, such as  $-\text{OH}$ ,  $-\text{C}=\text{O}$ ,  $-\text{COOH}$  and  $-\text{C}-\text{O}-\text{C}$ , which provide a unique platform for the binding of other substances [6–8].

Recently, with the development of ND synthesis techniques, the application of ND in electrochemistry has been widely reported. Simioni et al. [9] constructed an ND-based electrochemical sensor and successfully used it in determining a pyrazinamide antibiotic. Camargo et al. [10] introduced an electrochemical biosensor with tyrosinase immobilized in a matrix of NDs and potato starch; the sensor was suitable for the detection of catechol. Peltola et al. [11] combined NDs with tetrahedral amorphous carbon thin films in coatings on a Ti-coated Si-substrate; the NDs substantially enhanced its dopamine detection performance. ND modification has been reported to not affect the electrochemical performance of bare electrodes; on the contrary, it would substantially increase its electrochemical specific surface area and surface electron transfer rate [12]. Moreover, ND is chemically stable, exhibits low adsorptivity, and does not react with any acid or alkali, enabling ND to effectively prevent the passivation and improve the lifetime of an electrode.

Sulfonamides are a class of drugs with p-aminobenzene sulfonamide structure. They are widely used as anti-inflammatory drugs and animal feed additives and in the treatment of animal diseases [13–15]. However, sulfonamides have several serious side effects on the human body, including potential teratogenic, carcinogenic, and mutagenic effects [16]. They not only enter the aquatic environment through animal excretion and wastewater discharge, but also enter the human body through the food chain, thereby posing a serious threat to both the ecological environment and human health [17,18]. Thus far, many countries have established a maximum residue limit of sulfonamides in animal-derived food and feed of  $100\ \mu\text{g}/\text{kg}$  [19]. Common methods for the determination of sulfonamides include UV-visible spectrophotometry [20], high-performance liquid chromatography [21,22], and high-performance liquid chromatography tandem mass spectrometry [23,24]. Although these methods are highly accurate, they have a number of disadvantages, including complex pretreatment processes, slow detection speeds, and high detection costs, making them unsuitable for the rapid detection of a large number of samples. Comparatively, because of its simple equipment setup, simple operation, high sensitivity, fast analysis speed, and low cost, electrochemical detection is more suitable in the field of rapid detection [25,26].

In this study, a simple ND modification method of a glassy carbon electrode (GCE) is introduced and the influence of the amount of ND is studied. Its electrochemical performance, including its electroactive surface area and electron transfer rate, are investigated, and the results are compared with those obtained with a bare GCE. Sulfanilamide is chosen as a representative sulfonamide, and the square wave voltammetry (SWV) technique is used to detect the concentration of sulfanilamide solutions. A comparative study of the electrochemical detection of sulfanilamide on a GCE and on ND-modified GCE (GCE–ND) under optimum conditions is conducted.

## 2. EXPERIMENTAL

### 2.1 Reagents and Materials

ND powder with a grain size smaller than 10 nm was purchased from Aladdin Industrial Corporation (Shanghai, China). GCEs ( $d = 5$  mm), a Ag/AgCl electrode (in  $3.0 \text{ mol}\cdot\text{L}^{-1}$  KCl solution), and a Pt wire electrode were purchased from Chuxi Industrial Corporation (Shanghai, China). Sulfanilamide was purchased from Sinopharm Chemical Reagent Corporation. All chemical reagents were analytical grade. All aqueous solutions were prepared with ultrapure water (resistivity  $< 18 \text{ M}\Omega\cdot\text{cm}$ ). On the basis of a literature method [27,28], the sulfanilamide solution was prepared by dissolving sulfanilamide in HAc–NaAc buffer solution ( $\text{pH} = 4.5$ ).

### 2.2 Instruments

All ultrasonic baths were operated in UltraCleaner JT 410HT (Jietuo, China), including for the dispersion of the ND and the pretreatment of the GCEs. Morphological analysis was conducted by scanning electron microscopy (FEI-Scios 2 Hivac, USA). The crystalline structure of ND was analyzed by Raman spectroscopy using a 532 nm laser (Thermo Fischer DXR, USA). Cyclic voltammetric analysis and square wave voltammetric analysis were both carried out with an electrochemical workstation (CHI 660E, Chenhua, China) using a three-electrodes system in which a GCE or GCE-ND, a Ag/AgCl electrode, and a Pt wire electrode were used as the working electrode, reference electrode, and the counter electrode, respectively.

### 2.3 Modification of GCE

Each GCE was pretreated as follows: First, it was mechanically polished with alumina powder and rinsed with ultrapure water thoroughly. Second, the GCE was ultrasonically washed in an ultrapure water bath for 3 min; this procedure was repeated three times. Third, the GCE was ultrasonically washed for 2 min in 1:1  $\text{HNO}_3$  solution, 1:1 ethanol solution, and ultrapure water, in turn. Fourth, three additional ultrasonic water bath cleaning procedures were conducted before the electrode was air dried at room temperature. Finally, to oxidize the top carbon layer to enhance conductivity, the GCE was activated by cyclic voltammetry (CV) analysis repeatedly in  $0.5 \text{ mol}\cdot\text{L}^{-1}$   $\text{H}_2\text{SO}_4$  solution over the scanning from  $-1.0$  to  $1.0$  V until a stable cyclic voltammetric curve was attained.

A stable and uniformly dispersed ND suspension was prepared by adding 10 mg of ND powder into 250 mL of ultrapure water and ultrasonically treating the resultant mixture for 1 h. The obtained suspension was sealed, each time before use, it was ultrasonicated for 20 min to ensure that the ND was uniformly dispersed.

The GCEs were modified as follows: a certain amount of ND suspension droplets were added to the surface of a GCE, which was kept stationary and allowed to dry naturally. The obtained modified GCE is termed as the GCE–ND.

## 2.4 Electrochemical Measurements

The electrochemical performance of the bare GCE and the GCE–ND was characterized by CV analysis with the  $[\text{Fe}(\text{CN})_6]^{3-}$  redox couple. A volume of 50 mL of  $3 \text{ mmol}\cdot\text{L}^{-1}$   $\text{K}_3[\text{Fe}(\text{CN})_6]$  in  $0.1 \text{ mol}\cdot\text{L}^{-1}$  KCl solution was added to a glass electrochemical cell, and the scan rate was maintained at  $50 \text{ mV}\cdot\text{s}^{-1}$  while the potential was varied from  $-0.4$  to  $0.6 \text{ V}$ . In addition, the electroactive surface area and heterogeneous electron transfer rate constant of both electrodes were obtained from a set of CV analyses conducted under different scan rates.

The electroactive surface area was calculated using the Randles-Sevcik equation:

$$I_p = \pm(2.69 \times 10^5)n^{3/2}AD^{1/2}Cv^{1/2} \quad (1)$$

where  $I_p$  is the anodic or cathodic peak current ( $\mu\text{A}$ ),  $n$  is the number of electrons transferred ( $n = 1$ ),  $A$  is the electroactive surface area ( $\text{cm}^2$ ),  $D$  is the diffusion coefficient ( $D = 7.6 \times 10^{-6} \text{ cm}^2\cdot\text{s}^{-1}$  for  $\text{K}_3[\text{Fe}(\text{CN})_6]$  in  $0.1 \text{ mol}\cdot\text{L}^{-1}$  KCl solution),  $C$  is the redox couple concentration ( $3.0 \times 10^{-6} \text{ mol}\cdot\text{cm}^{-3}$ ), and  $v$  is the scan rate ( $\text{V}\cdot\text{s}^{-1}$ ).

The heterogeneous electron transfer rate constant was calculated using the Nicholson equation:

$$k^0 = \Psi[\pi D n v F / (RT)]^{1/2} \quad (2)$$

where  $k^0$  is the heterogeneous electron transfer rate constant ( $\text{cm}\cdot\text{s}^{-1}$ ),  $\Psi$  is the dimensionless kinetic parameter that can be calculated from the equation proposed by Lavagnini et al [29],  $F$  is the Faradays constant ( $96485 \text{ C}\cdot\text{mol}^{-1}$ ),  $R = 8.314 \text{ J}\cdot\text{K}\cdot\text{mol}^{-1}$ ,  $T \approx 298.15 \text{ K}$ , and other parameters are as previously defined.

The electrochemical detection of sulfanilamide on both bare GCE and GCE–ND was also determined by CV analysis with a scan rate of  $50 \text{ mV}\cdot\text{s}^{-1}$  and potentials varying from  $0.8$  to  $1.3 \text{ V}$ . The detection of sulfanilamide was conducted by SWV over a potential range of  $0.6$ – $1.3 \text{ V}$ ; the potential pulse amplitude, potential increment, and frequency were considered as key parameters to confirm optimum conditions. During detection, each sample was measured three times to ensure the accuracy and repeatability of the measurement. The limit of detection was determined using the ratio of  $3s/m$ , where  $m$  is the slope of the linear detection calibration curve and  $s$  is the standard deviation value of the anodic peak currents of ten blank samples [30].

## 3. RESULTS AND DISCUSSION

### 3.1 Characterization of GCE–ND

The effect of the ND content on the surface morphology and electrochemical performance of the GCE–NDs was studied first. SEM observations of surfaces of GCEs modified with different ND suspension volumes are shown in Fig. 1. When the volume of ND solution was less than  $100 \mu\text{L}$ , a large number of evenly distributed nanosized ND particles were detected. However, with increasing of ND suspension volume, the agglomeration effect of ND particles was substantially enhanced [31]. When the ND suspension volume was  $200 \mu\text{L}$ , stacked ND clusters instead of clearly dispersed ND particles were mainly observed and their diameter even reached approximately  $4 \mu\text{m}$ . Obviously, the ND with a small

grain size and good dispersion led to larger specific surface areas, providing more electroactive surface areas and possibly better electrochemical performance.

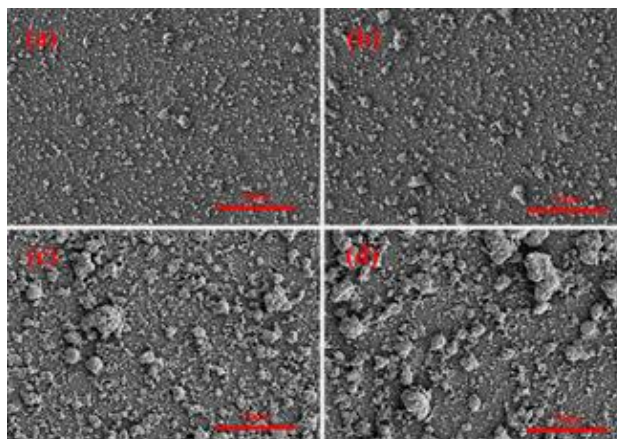


**Figure 1.** SEM images of GCE surfaces modified with different volumes of an ND suspension: (a) 50  $\mu\text{L}$  of ND suspension; (b) 100  $\mu\text{L}$  of ND suspension; (c) 150  $\mu\text{L}$  of ND suspension; and (d) 200  $\mu\text{L}$  of ND suspension.

Furthermore, CV analyses with the  $[\text{Fe}(\text{CN})_6]^{3-}$  redox couple were carried out to study the difference in the electrochemical performance of the various GCE–NDs. The cyclic voltammograms obtained under scan rates ranging 10–120  $\text{mV}\cdot\text{s}^{-1}$  using GCEs modified with different volumes of ND are displayed in Fig. 2a–d. The corresponding variation of the anodic and cathodic peak current values under different scan rates were collected and are displayed in Fig. 2e. Under all of the investigated conditions, linear relationships were clearly observed between both anodic and cathodic currents and the square root of the scan rate, indicating that the reactions were all controlled by diffusion [32].

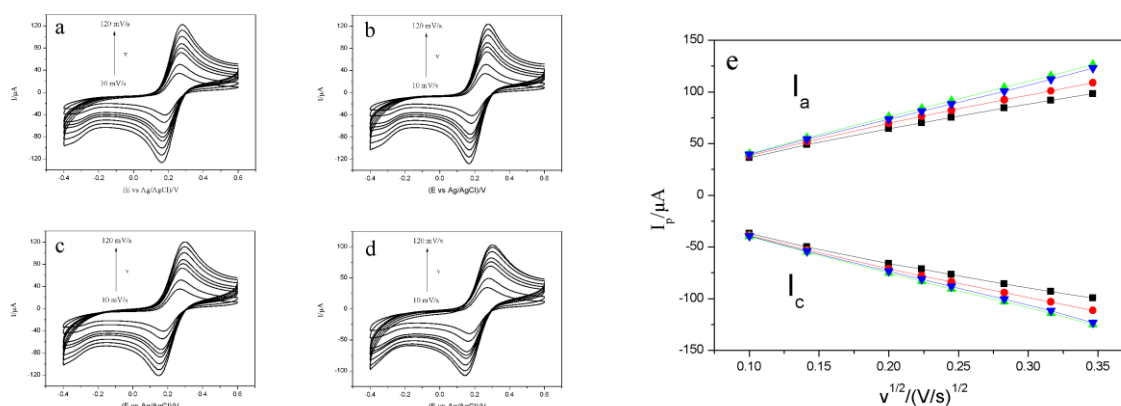


**Figure 2.** (a–d) CV curves recorded under scan rates ranging 10–120  $\text{mV}\cdot\text{s}^{-1}$  using GCE modified with different volumes of ND: (a) 50  $\mu\text{L}$  of ND suspension; (b) 100  $\mu\text{L}$  of ND suspension; (c) 150  $\mu\text{L}$  of ND suspension; (d) 200  $\mu\text{L}$  of ND suspension. (e) The variation of anodic and cathodic peak current values versus the square root of the scan rate, as obtained from CV analyses with GCEs modified with different volumes of ND suspension: ▼: 50  $\mu\text{L}$  of ND suspension, ▲: 100  $\mu\text{L}$  of ND suspension, ●: 150  $\mu\text{L}$  of ND suspension, ■: 200  $\mu\text{L}$  of ND suspension. Solution: 3  $\text{mmol}\cdot\text{L}^{-1}$   $\text{K}_3[\text{Fe}(\text{CN})_6]$  in 0.1  $\text{mol}\cdot\text{L}^{-1}$  KCl solution.

In addition, electroactive surface areas were calculated using Eq. 1 as 0.151, 0.157, 0.128, and 0.112 cm<sup>2</sup> for GCEs modified with 50, 100, 150, and 200 μL of ND suspension, respectively. The GCE modified with 100 μL of ND suspension clearly exhibited the largest electroactive surface area, which also confirms that the agglomeration of ND particles adversely affected its electrochemical performance. Thus, 100 μL of the ND suspension was considered as the optimum modification condition and was used in subsequent experiments.

To analyze the structural bonding configuration of the GCE–ND, Raman spectral analysis was conducted; the results are shown in Fig. 3. Two typical characteristic ND Raman peaks at ~1350 cm<sup>-1</sup> (D band) and ~1580 cm<sup>-1</sup> (G band) are observed; these peaks correspond to the lattice defects of carbon atoms and the stretching of *sp*<sup>2</sup> carbon in the grain boundary, respectively [33]. Another broad symmetrical peak at ~2650 cm<sup>-1</sup> (2D band), which represents the overtone of the transverse optical D band [34], was also found.

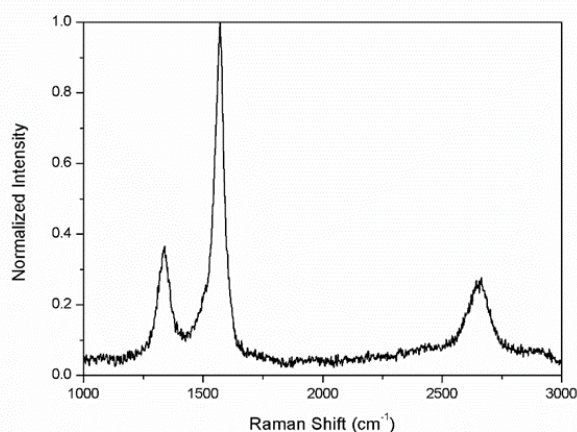


**Figure 3.** Raman spectrum of the surface of the GCE modified with 100 μL of ND suspension.

### 3.2 Electrochemical Behaviors of GCE and GCE–ND

The electrochemical performances of the bare GCE and GCE–ND were investigated by CV analyses using the [Fe(CN)<sub>6</sub>]<sup>3-</sup> redox couple under a scan rate of 50 mV·s<sup>-1</sup>; the results are shown in Fig. 4. The cyclic voltammograms presented in Fig. 4c show that the GCE–ND had a substantially higher anodic peak current (84.16 μA for the GCE–ND, and 46.68 μA for the bare GCE) and a lower cathodic peak current (-83.40 μA for the GCE–ND, and -49.00 μA for the bare GCE) than the bare GCE. In addition, the GCE–ND also showed a lower peak potential difference (99 mV for the GCE–ND, and 207 mV for the bare GCE). These results indicate that the GCE–ND exhibited remarkably superior electrochemical performance compared with the bare GCE.

CV analyses under different scan rates ranging 10–120 mV·s<sup>-1</sup> using the bare GCE and GCE–ND were carried out (Fig. 4a and 4b); the corresponding variations in the peak current values are shown in Fig. 4d. Two linear relationships are observed between the peak currents and the square root of the scan rates for both electrodes. Their electroactive surface areas and heterogeneous electron transfer

rate constants were calculated using Eq. 1 and Eq. 2, respectively; the results are listed in Table 1. After ND modification, the electroactive surface area increased from 0.0744 cm<sup>2</sup> to 0.157 cm<sup>2</sup>, and the heterogeneous electron transfer rate constant also increased from 0.000915 cm·s<sup>-1</sup> to 0.00462 cm·s<sup>-1</sup>. These results further confirm that the ND modification substantially enhanced the electrochemical performance of the bare GCE, thereby demonstrating ND's potential application in electrochemical detection.

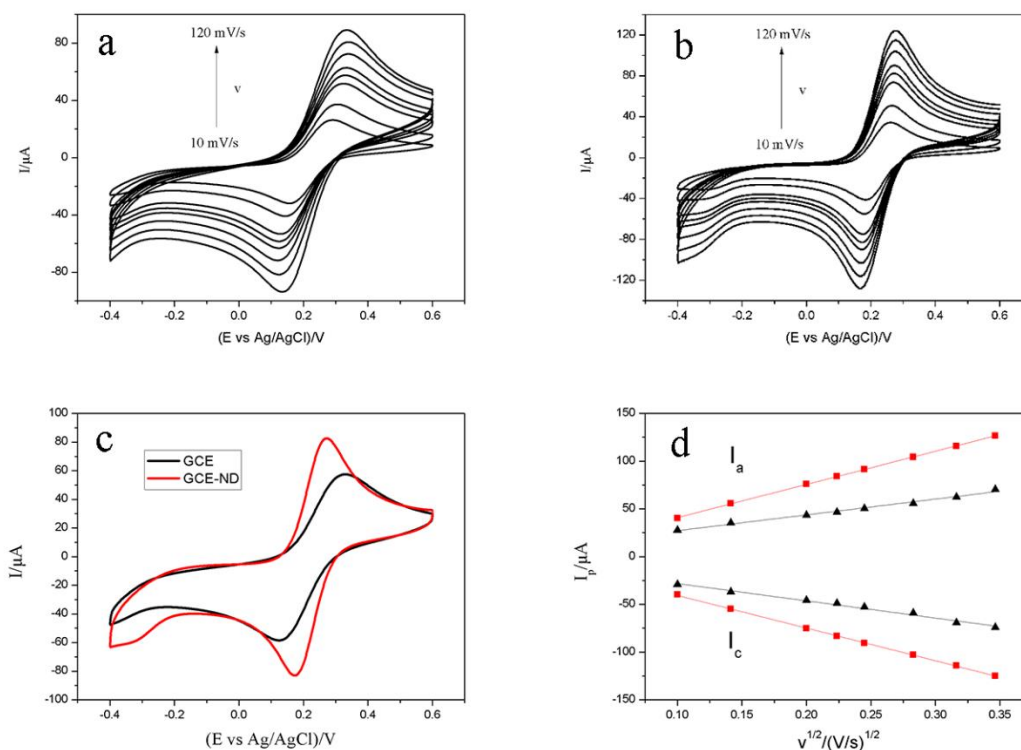


**Figure 4.** (a-b) Cyclic voltammograms under scan rates ranging 10–120 mV·s<sup>-1</sup>, as recorded using the (a) bare GCE and (b) GCE–ND. (c) Comparative CV curves obtained using the bare GCE and GCE–ND as working electrodes under a scan rate of 50 mV·s<sup>-1</sup>. (d) The variations in the anodic and cathodic peak current values versus the square root of the scan rate obtained from CV analyses under different scan rates on the bare GCE and GCE–ND. (▲: GCE, ■: GCE–ND). Solution: 3 mmol·L<sup>-1</sup> K<sub>3</sub>[Fe(CN)<sub>6</sub>] in 0.1 mol·L<sup>-1</sup> KCl solution.

**Table 1.** Calculated electroactive surface area and heterogeneous electron transfer rate constant for the bare GCE and GCE–ND.

Electrode	Electroactive Surface Area (cm <sup>2</sup> )	Heterogeneous Electron Transfer Rate Constant (cm·s <sup>-1</sup> )
GCE	0.0744	0.000915
GCE–ND	0.157	0.00462



### 3.3 Electrochemical Response of Sulfanilamide

CV analyses of  $50 \text{ mg}\cdot\text{L}^{-1}$  sulfanilamide on both the bare GCE and GCE-ND were conducted; the results are displayed in Fig. 5. Obvious oxidation peaks are observed in both curves, whereas no reduction peaks are evident. For the bare GCE, the oxidation peak potential was  $1.076 \text{ V}$  and the peak current was  $9.13 \text{ }\mu\text{A}$ ; by contrast, for the GCE-ND, they were  $1.058 \text{ V}$  and  $10.26 \text{ }\mu\text{A}$ , respectively. This difference is due to the larger electroactive surface area of the GCE-ND, which enables a greater number of electrode reactions on the surface of the electrode. Moreover, the electron transfer rate between the electroactive material and the surface of the electrode greatly increased after the modification with ND, resulting in an increase in the oxidation peak current of sulfanilamide on the GCE-ND and in a negative shift of the peak potential. Notably, after the ND modification, the electroactive surface area increased by 111%, whereas the oxidation peak current from the CV analysis of sulfanilamide increased only 12%. This difference might be attributed to the oxidation of sulfanilamide being an electropolymerization oxidation reaction, which is a diffusion-controlled irreversible electrode reaction process [28].

The aforementioned results are further supported by SWV analysis using the same solution, where the current responses on the bare GCE and GCE-ND were  $35.53 \text{ }\mu\text{A}$  and  $54.16 \text{ }\mu\text{A}$ , respectively. The current response of the GCE-ND increased only 52%, which is less than the increase of the electroactive surface area. These results indicate that the GCE-ND shows better performance than the bare GCE in the electrochemical detection of sulfanilamide.

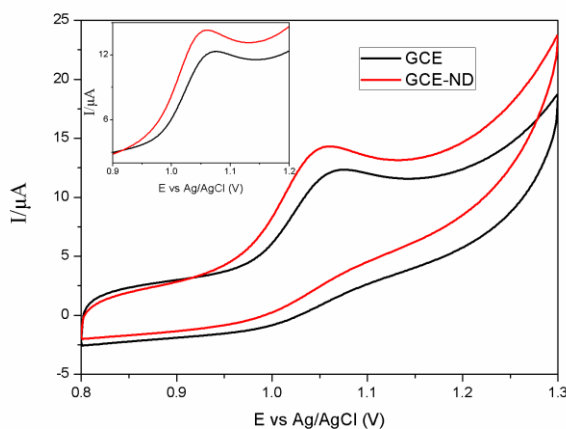


**Figure 5.** Cyclic voltammograms of  $50 \text{ mg}\cdot\text{L}^{-1}$  sulfanilamide in HAc–NaAc buffer solution ( $\text{pH} = 4.5$ ) on the bare GCE and GCE-ND, as recorded at a scan rate of  $50 \text{ mV}\cdot\text{s}^{-1}$  and over a potential range  $0.8\text{--}1.3 \text{ V}$ . Inset: variation in the anodic oxidation peak currents over the potential range  $0.9\text{--}1.2 \text{ V}$ , as obtained from cyclic voltammograms.

### 3.4 Optimization of the SWV Technique

The SWV technique has high sensitivity and has already been widely used in the detection of sulfonamides [35,36]. Thus, it was selected for sulfanilamide detection in this work; the detection parameters were optimized first. The accumulation process has been reported to strongly affect SWV



detection [37,38]. Therefore, the effect of accumulation potential and time on the detection of sulfanilamide was investigated using the bare GCE. When the accumulation potential ranged 0.6–1.3 V, the anodic oxidation peak current reached its highest value at 0.7 V. Furthermore, when the accumulation time ranged 0–300 s, the peak current increased with increasing accumulation time from the beginning, reached its maximum at 180 s, and remained stable thereafter. To achieve a greater peak current, an accumulation potential of 0.7 V and accumulation time of 180 s were selected as optimum conditions and used in subsequent experiments.

In the SWV technique, the potential pulse amplitude ( $a$ ), step potential ( $\Delta E_s$ ), and frequency ( $f$ ) have often been considered as key parameters in determining the optimum conditions. Thus, these parameters were investigated in the following ranges for the detection of sulfanilamide solution using the bare GCE:  $1 \text{ mV} \leq \Delta E_s \leq 7 \text{ mV}$ ,  $10 \text{ mV} \leq a \leq 90 \text{ mV}$ , and  $10 \text{ Hz} \leq f \leq 50 \text{ Hz}$ . The optimum conditions for each parameter depended on the maximum anodic oxidation peak current; the optimum parameters were  $\Delta E_s = 4 \text{ mV}$ ,  $a = 70 \text{ mV}$ , and  $f = 40 \text{ Hz}$ , respectively.

### 3.5 Sulfanilamide Detection on Bare GCE and GCE–ND

Under optimum conditions, the detections of sulfanilamide by the SWV technique using the bare GCE and GCE–ND were carried out; the results are recorded in Fig. 6. As shown in Fig. 6a, the anodic peak current increased substantially with increasing sulfanilamide concentration. The variation in the anodic peak currents under different sulfanilamide concentrations is displayed in the inset of Fig. 6a, which shows a linear range of  $1\text{--}80 \text{ mg}\cdot\text{L}^{-1}$ , as expressed by equation  $I_p(\mu\text{A}) = 3.286 + 0.8358C(\text{mg}\cdot\text{L}^{-1})$  ( $R^2 = 0.9994$ ). According to the method described in section 2.4, the calculated limit of detection with the bare GCE is  $0.744 \text{ mg}\cdot\text{L}^{-1}$ .

Fig. 6b shows the result of sulfanilamide detection using the GCE–ND. From the analytical peak current curve in the inset of Fig. 6b, a linear range of  $0.2\text{--}100 \text{ mg}\cdot\text{L}^{-1}$  with expression of equation  $I_p(\mu\text{A}) = 4.829 + 0.9804C(\text{mg}\cdot\text{L}^{-1})$  ( $R^2 = 0.9949$ ) is observed. The calculated limit of detection with the GCE–ND is  $0.161 \text{ mg}\cdot\text{L}^{-1}$ , which is as much as 78.4% lower than that of the bare GCE. Clearly, the ND modification greatly extends the linear detection range of the bare GCE and reduces its detection limit. These effects might be due to the increase of the electroactive surface area and the heterogeneous electron transfer rate constant caused by the ND modification. Taken together, ND modification strongly benefits the electrochemical detection of sulfanilamide, resulting in a broader detection range and a lower detection limit.

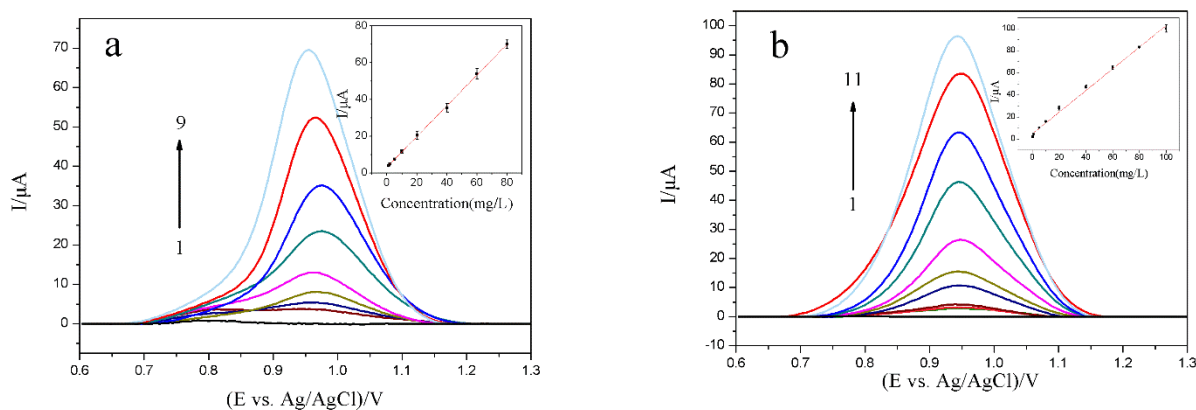


**Figure 6.** Square wave voltammograms of different sulfanilamide concentrations in HAC–NaAc buffer solution (pH = 4.5), as recorded using the bare GCE and GCE–ND under optimum conditions. Parameters:  $\Delta E_s = 4$  mV,  $a = 70$  mV, and  $f = 40$  Hz. Inset: variation in the anodic peak currents under different sulfanilamide concentrations. (a) Detection by the bare GCE, and sulfanilamide concentrations of (1) 0, (2) 1, (3) 2, (4) 5, (5) 10, (6) 20, (7) 40, (8) 60, and (9) 80 mg·L<sup>-1</sup>. (b) Detection by the GCE–ND, and sulfanilamide concentrations of (1) 0, (2) 0.2, (3) 0.5, (4) 1, (5) 5, (6) 10, (7) 20, (8) 40, (9) 60, (10) 80, and (11) 100 mg·L<sup>-1</sup>.

Table 2 lists several other methods for the electrochemical determination of sulfanilamide. With the exception of the molecularly imprinted polymer modification, which has a very low detection limit, the limit of detection achieved with other modification methods were of the same order of magnitude. The linear range achieved with the proposed ND modification method is similar or better than that achieved with other methods (Table 2). This result is attributed primarily to the ultra-high stability of ND, which broadens the electrode's linear range [43,44]. Moreover, the modification technique proposed in the present work is simple compared with the techniques associated with other methods.

**Table 2.** Comparison of different methods for the electrochemical determination of sulfanilamide

Electrode	Linear Range ( $\mu\text{mol}\cdot\text{L}^{-1}$ )	LOD ( $\mu\text{mol}\cdot\text{L}^{-1}$ )	Ref.
OPPy/PGE	25–1000	1.53	[39]
GCE	5.0–74.7	3.1	[35]
Carboxyl/MWCNTs/DMF/GCE	1–100	0.5	[40]
MWCNTs/GCE	0.58–58.1	0.058	[41]
Gr/AuNPs/GCE	0.1–1000	0.011	[42]
MIP/GO/GCE	0.058–5.81	–	[28]
GCE–ND	1.2–581.4	0.94	This work

Abbreviations:

LOD – Limit of detection; OPpy – Overoxidized polypyrrole; PGE – Pencil graphite electrode; MWCNTs – Multiwalled carbon nanotubes; DMF – Dimethyl formamide; Gr – Graphene; AuNPs – Au nanoparticles; MIP – Molecularly imprinted polymer; GO – Graphene oxide

### 3.6 Detection Accuracy of Bare GCE and GCE-ND

The detection accuracy of sulfanilamide using the SWV technique on both bare GCE and GCE-ND was verified using interday repeatability studies. Sulfanilamide solutions with concentrations of 15, 25, 35, 45, and 55 mg·L<sup>-1</sup> were prepared; the test results are displayed in Table 3. For each concentration, three successive SWV measurements were carried out, and corresponding average relative standard deviations (RSDs) of 1.92% and 2.54% were obtained for the bare GCE and GCE-ND, respectively. Thus, the SWV technique shows good repeatability with both electrodes.

The detection accuracy of both electrodes was also investigated. For the bare GCE, the relative error of detection increased with increasing concentration and the average relative error was 5.33%. By contrast, for the GCE-ND, the relative error remained relatively stable and the average relative error was only 3.43%, which implies that the GCE-ND exhibited greater detection accuracy than the bare GCE. In summary, sulfanilamide detection using the SWV technique on the GCE-ND exhibited greater repeatability and accuracy than detection using the same technique on the bare GCE.

**Table 3.** Interday detection of sulfanilamide using SWV technique on both bare GCE and GCE-ND under optimum conditions. Parameters:  $\Delta E_s = 4$  mV,  $a = 70$  mV and  $f = 40$  Hz.

Electrode	Sulfanilamide concentration		Relative error (%)
	Added (mg·L <sup>-1</sup> )	Detected (mg·L <sup>-1</sup> )	
GCE	15.00	15.25±0.83	1.67
	25.00	25.67±0.34	2.68
	35.00	37.15±0.34	6.14
	45.00	42.09±0.74	6.47
	55.00	60.33±0.08	9.69
GCE-ND	15.00	15.02±0.83	0.13
	25.00	26.64±0.69	6.56
	35.00	36.53±0.85	4.37
	45.00	43.51±0.62	3.31
	55.00	56.52±0.47	2.76

## 4. CONCLUSION

A comparative study of the electrochemical performances of the bare GCE and GCE-ND and their applications in sulfanilamide detection was presented in this work. The volume of ND suspension strongly influenced the electrochemical performance of the electrodes. With increasing volume of ND suspension, the agglomeration effect became serious, substantially decreasing the electroactive surface area. In this work, 100  $\mu$ L of ND suspension (40 mg·L<sup>-1</sup>) was found to be the optimum modification condition. Subsequently, the electrochemical performance of the bare GCE and GCE-ND was compared by CV analyses using a [Fe(CN)<sub>6</sub>]<sup>3-</sup> redox couple. The results showed that the electroactive surface area and heterogeneous electron transfer rate constant of the GCE-ND were 2.11 and 5.05 times higher, respectively, than those of the GCE. In the electrochemical detection of sulfanilamide solution using the SWV technique, the GCE-ND showed a broader linear dynamic range of 0.2–100 mg·L<sup>-1</sup> with a

detection limit of  $0.161 \text{ mg}\cdot\text{L}^{-1}$ ; the detection limit was as much as 78.4% lower than that of the bare GCE. Furthermore, the interday detection experiments revealed that the GCE–ND also exhibited greater repeatability and accuracy. This study demonstrates ND's potential application in the voltammetric detection of sulfanilamide.

#### ACKNOWLEDGEMENTS

The authors gratefully acknowledge the financial support from Ningbo Natural Science Foundation (Grant No. 2018A610280), and Ningbo Polytechnic High-level Talents Introduction Research Project (Grant No. RC201708). The authors also gratefully thank Scientific Compass for conducting SEM and Raman spectrum analyses.

#### References

1. T. Laurila, S. Sainio and M.A. Caro, *Prog. Mater. Sci.*, 88 (2017) 499.
2. A. Rana, N. Baig and T.A. Saleh, *J. Electroanal. Chem.*, 833 (2019) 313.
3. P. Yáñez-Sedeño, J.M. Pingarrón, J. Riu and F.X. Rius, *TrAC Trend Anal. Chem.*, 29 (2010) 939.
4. X.Y. Ma, M.F. Chen, X. Li, A. Purushothaman and F.C. Li, *Int. J. Electrochem. Sci.*, 4 (2012) 1687.
5. X.Y. Wu, L.L. Liu, Z.Q. Xie and Y.G. MA, *Chem. J. Chinese Univ.*, 37 (2016) 409.
6. A. Krueger and D. Lang, *Adv. Funct. Mater.*, 22 (2012) 890.
7. N. Nunn, M. Torelli, G. McGuire and O. Shenderova, *Curr. Opin. Solid State Mater. Sci.*, 21 (2017) 1.
8. N.J. Yang, J.S. Foord and X. Jiang, *Carbon*, 99 (2016) 90.
9. N.B. Simioni, T.A. Silva, G.G. Oliveira and O. Fatibello-Filho, *Sensor Actuat. B Chem.*, 250 (2017) 315.
10. J.R. Camargo, M. Baccarin, P.A. Raymundo-Pereira, A.M. Campos, G.G. Oliveira, O. Fatibello-Filho, O.N.Jr. Oliveira and B.C. Janegitz, *Anal. Chim. Acta*, 1034 (2018) 137.
11. E. Peltola, N. Wester, K.B. Holt, L.S. Johansson, J. Koskinen, V. Myllymäki and T. Laurila, *Biosens. Bioelectron.*, 88 (2017) 273.
12. K.B. Holt, C. Ziegler, D.J. Caruana, J.B. Zang, E.J. Millán-Barrios, J.P. Hu and J.S. Foord, *Phys. Chem. Chem. Phys.*, 10 (2007) 303.
13. A. El-Ghenymy, N. Oturan, M.A. Oturan, J.A. Garrido, P.L. Cabot, F. Centellas, R.M. Rodríguez and E. Brillas, *Chem. Eng. J.*, 234 (2013) 115.
14. Y. Feng, C.Z. Liao and K. Shih, *Chemosphere*, 154 (2016) 573.
15. W.Y. Zhu, J.C. Liu, S.Y. Yu, Y. Zhou and X.L. Yan, *J. Hazard. Mater.*, 318 (2016) 407.
16. W. Baran, E. Adamek, J. Ziemiańska and A. Sobczak, *J. Hazard. Mater.*, 196 (2011) 1.
17. J.B. Chen, X.F. Zhou, Y.L. Zhang and H.P. Gao, *Sci. Total Environ.*, 432 (2012) 269.
18. R.C. Zhang, Y.K. Yang, C.H. Huang, L. Zhao and P.C. Sun, *Water Res.*, 103 (2016) 283.
19. H. Sereshti, M. Khosraviani and M.S. Amini-Fazl, *Talanta*, 121 (2014) 199.
20. S.A. Errayess, A.A. Lahcen, L. Idrissi, C. Marcoaldi, S. Chiavarini and A. Amine, *Spectrochim. Acta Part A Mol. Biomol. Spectrosc.*, 181 (2017) 276.
21. I.G. Casella, M. Contursi and D. Gioia, *Electroanal.*, 24 (2012) 2125.
22. Q.X. Zhou and Z. Fang, *Talanta*, 141 (2015) 170.
23. C. Nebot, P. Regal, J.M. Miranda, C. Fente and A. Cepeda, *Food Chem.*, 141 (2013) 2294.
24. H.J. Kim, M.H. Jeong, H.J. Park, W.C. Kim and J.E. Kim, *Food Chem.*, 196 (2015) 1144.
25. T. Yang, R.Z. Yu, Y.H. Yan, H. Zeng, S.Z. Luo, N.Z. Liu, A. Morrin, X.L. Luo and W.H. Li, *Sensor Actuat. B Chem.*, 274 (2018) 501.

26. G. Maduraiveerana and W. Jin, *Trends Environ. Anal. Chem.*, 13 (2017) 10.
27. M. Arvand, R. Ansari and L. Heydari, *Mater. Sci. Eng. C*, 31 (2011) 1819.
28. X.B. Wei, X.H. Xu, W. Qi, Y. Wu and L.H. Wang, *Prog. Nat. Sci. Mater. Int.*, 27 (2017) 374.
29. I. Lavagnini, R. Antiochia and F. Magno, *Electroanal.*, 16 (2004) 505.
30. D.C. Harris, *Quantitative Chemical Analysis*, W.H. Freeman & Company, (2015), USA.
31. M. Khan, A.A. Khurram, T.H. Li, T.K. Zhao, C.Y. Xiong, Z. Ali, N. Ali and A. Ullah, *Diam. Relat. Mater.*, 78 (2017) 58.
32. P.K. Brahman, L. Suresh, V. Lokesh and S. Nizamuddin, *Anal. Chim. Acta*, 917 (2016) 107.
33. M. Mermoux, S. Chang, H.A. Girard and J.C. Arnault, *Diam. Relat. Mater.*, 87 (2018) 248.
34. S. Gupta and J. Farmer, *J. Appl. Phys.*, 109 (2011) 014314.
35. B.R.L. Ferraz, T. Guimarães, D. Profeti and L.P.R. Profeti, *J. Pharm. Anal.*, 8 (2018) 55.
36. H. Chasta and R.N. Goyal, *Electroanal.*, 27 (2015) 1229.
37. L.R. Yang, S.J. Zhou, Y.Z. Xiao, Y.F. Tang and T.Y. Xie, *Food Chem.*, 188 (2015) 446.
38. S.G. Dmitrienko, E.V. Kochuk, V.V. Apyari, V.V. Tolmacheva and Y.A. Zolotov, *Anal. Chim. Acta*, 850 (2014) 6.
39. S.P. Ozkorucuklu, L. Ozcan, Y. Sahin and G. Alsancak, *Aust. J. Chem.*, 64 (2011) 965.
40. B.S. He and W.B. Chen, *Int. J. Electrochem. Sci.*, 10 (2014) 4335.
41. A.M. Bueno, A.M. Contento and Á. Ríos, *Anal. Methods*, 5 (2013) 6821.
42. B.S. He and X.H. Yan, *Sensors*, 18 (2018) 846.
43. L.Y. Jiang, I. Santiago and J.S. Foord, *Chem. Commun.*, 1 (2018) 43.
44. D.J.E. Costa, J.C.S. Santos, F.A.C. Sanches-Brandão, W.F. Ribeiro, G.R. Salazar-Banda and M.C.U. Araujo, *J. Electroanal. Chem.*, 789 (2017) 100.